Analysis of Fast Decoupled Power Flow via Multiple Axis Rotations

Paprapee Buason, Daniel K. Molzahn
School of Electrical and Computer Engineering
Georgia Institute of Technology
Atlanta, GA, USA
{pbuason6, molzahn}@gatech.edu

***Abstract*—The Fast Decoupled Power Flow (FDPF) method has been widely adopted due to its computational speed advantages relative to the Newton-Raphson method for many practically relevant power flow problems. The FDPF method relies on the assumption that the lines are highly inductive, i.e., have small R/X ratios. When this assumption does not hold (e.g., for distribution systems and some subtransmission systems), the FDPF method may exhibit slow convergence or fail to converge entirely. To address such cases, previous work has proposed an *axis rotation* method which rescales the complex power injections and the bus admittances by a unit-magnitude complex scalar parameter. Since this complex parameter adjusts the lines' R/X ratios, an appropriate choice for this parameter can improve the FDPF method's performance. In contrast to previous work that only introduces one complex parameter for the entire system (or one complex parameter per large subsystem), we propose and analyze an axis rotation method that introduces different complex parameters at each bus. The additional degrees of freedom provided in this more granular approach are particularly valuable for systems where the lines have wider ranges of R/X ratios. To obtain appropriate values for the complex parameters, we propose to minimize the sum of the squared errors associated with the FDPF approximations. This method can also be adapted for cases with large voltage angle differences. Our simulation results demonstrate the effectiveness of the proposed method.**

***Index Terms*—Fast Decoupled Power Flow, Axis Rotation, Theta Compensation.**

I. Introduction

Power flow computations are essential tools for many power system analyses (e.g., contingency screening, expansion planning, initializing dynamic simulations, etc.). Since the power flow equations are nonlinear, iterative methods are typically used to compute the unknown states, e.g., voltage magnitudes and angles. The Fast Decoupled Power Flow (FDPF) is a widely used iterative power flow solution method that has computational speed advantages for many problems [1].

The FDPF method assumes that the lines' series resistances and shunt reactances are negligible and that the angle differences between connected buses are small. Based on these assumptions, the FDPF method derives constant matrices that are used in each iteration and thus only need to be factorized once. However, some systems like distribution systems and certain subtransmission systems have highly resistive lines, which, in turn, worsen the FDPF method's convergence performance. Joint analyses of these systems with transmission systems are crucial due to the ongoing increase in distributed energy resources in distribution and subtransmission systems.

Previous research efforts have analyzed the convergence performance of the FDPF method. Convergence conditions for the FDPF method and an upper bound on the error at each iteration are presented in [2]. Prior work in [3] explores how the FDPF method's performance is affected when the lines' series resistances and shunt reactances are not neglected. The authors in [3] also emphasize that large R/X ratios lead to slow convergence or failure of the FDPF method.

Researchers have proposed methods for improving the FDPF method's performance in systems with high R/X ratios using the concept of *axis rotation* [4], [5]. Axis rotation normalizes the power flow equations using a unit-magnitude complex parameter. This concept is also framed as *complex per unit (cpu) normalization*, which introduces the axis rotation in terms of the base complex power and base admittance [6]–[9].

These concepts presented in previous work consider one axis rotation for an entire system or a subsystem. To the best of our knowledge, no prior work has applied different axis rotations at each bus in order to address various ranges of R/X ratios across a system. Hence, we aim to improve the FDPF method's convergence performance by exploiting the ability to choose different axis rotations at each bus. We also aim to efficiently and reliably apply our modified FDPF method to systems with lines that have widely varying R/X ratios.

We propose a method that pre-calculates all axis rotations in an offline manner for a given system topology and line impedances; thus, our method has limited computational requirements. The axis rotations at each bus are calculated by minimizing the sum of squared errors associated with the off-diagonal entries of the Jacobian matrix, which are approximated to zero in the traditional FDPF method.

The main contributions of this paper are:
(*i*) A FDPF formulation that permits distinct axis rotations at each bus along with a method for selecting appropriate values for these rotations.
(*ii*) An analysis of the axis rotations' impact on the convergence of the FDPF method in cases where the small angle difference and small R/X assumptions do not hold.
(*iii*) Numerical demonstrations of the axis rotations.

The rest of the paper is organized as follows. Section II provides background on the power flow equations and the

FDPF method. Section III discusses the FDPF method using axis rotations and the method to calculate the axis rotations at each bus. Section IV describes our numerical results. Section V concludes the paper and discusses future work.

II. Background

Consider an n-bus power system. The sets of buses and lines are $\mathcal{N} = \{1, \ldots, n\}$ and $\mathcal{L}$, respectively. Each bus is classified as either a slack bus with specified voltage magnitude and angle, typically $1\angle 0°$; a PV bus, which specifies the real power and the voltage magnitude; or a PQ bus, which specifies the real and reactive power. We define $\mathcal{N}_{i'} := \{k \,|\, (i,k) \in \mathcal{L}\}$ as the set of all buses that neighbor bus i. The set of bus i and its neighbors is denoted as $\mathcal{N}_i := \{k \,|\, (i,k) \in \mathcal{L}\} \cup \{i\}$. Subscript $(\cdot)_{ik}$ denotes that quantity from/connecting bus i to bus k. Subscript $(\cdot)_i$ denotes a quantity at bus i. The complex power injection at bus i, denoted as S_i, is:

$$S_i = V_i(\sum_{k \in \mathcal{N}_i} Y_{ik} V_k)^*, \tag{1}$$

where $V_i := |V_i| \angle \theta_i$ is the voltage phasor. The bus admittance is denoted as $Y_{ik} = G_{ik} + \mathbf{j} B_{ik}$, where G_{ik} (B_{ik}) is the conductance (susceptance). The asterisk symbol (*) denotes the complex conjugate, i.e., $(a + \mathbf{j}b)^* = a - \mathbf{j}b$, where $\mathbf{j} = \sqrt{-1}$. Other quantities written in bold are matrices. All quantities are given in per unit (pu) representation.

Subtracting the left hand side of (1) and taking real and imaginary parts yields the *power mismatch equations*, which indicate the mismatch between the calculated and specified power at bus i:

$$\Delta P_i = \sum_{k \in \mathcal{N}_i} |V_i||V_k|(G_{ik}\cos\theta_{ik} + B_{ik}\sin\theta_{ik}) - P_i, \tag{2a}$$

$$\Delta Q_i = \sum_{k \in \mathcal{N}_i} |V_i||V_k|(G_{ik}\sin\theta_{ik} - B_{ik}\cos\theta_{ik}) - Q_i, \tag{2b}$$

where P_i (Q_i) is the real (reactive) power injection from bus i, and $\theta_{ik} := \theta_i - \theta_k$ is the voltage angle difference between buses i and k. We define ΔP_i (ΔQ_i) as the real (reactive) power mismatch. Iterative algorithms such as the FDPF method attempt to compute the voltage magnitudes and angles by reducing the power mismatch to zero (within a specified tolerance).

The system of equations in (2a) and (2b) is nonlinear and differentiable. This system can be solved by the Newton-Raphson (NR) method [10]. The system of equations at the m^{th}-iteration, where $m \in \mathbb{Z}^+$, to solve this problem is:

$$\begin{bmatrix} \boldsymbol{\Delta\theta} \\ \boldsymbol{\Delta}|\boldsymbol{V}| \end{bmatrix}^m = -\boldsymbol{J}(\boldsymbol{\theta}^m, |\boldsymbol{V}|^m)^{-1} \begin{bmatrix} \boldsymbol{\Delta P} \\ \boldsymbol{\Delta Q} \end{bmatrix}^m, \tag{3}$$

where $\boldsymbol{J}$ is the Jacobian matrix for this system of equations:

$$\boldsymbol{J}(\boldsymbol{\theta}^m, \boldsymbol{V}^m) = \begin{bmatrix} \frac{\partial \boldsymbol{\Delta P}}{\partial \boldsymbol{\theta}} & \frac{\partial \boldsymbol{\Delta P}}{\partial |\boldsymbol{V}|} \\ \frac{\partial \boldsymbol{\Delta Q}}{\partial \boldsymbol{\theta}} & \frac{\partial \boldsymbol{\Delta Q}}{\partial |\boldsymbol{V}|} \end{bmatrix}^m. \tag{4}$$

The Jacobian matrix can be written in four separate blocks, as shown in (4). We update the voltage angles and magnitudes by: $\boldsymbol{\theta}^{m+1} = \boldsymbol{\theta}^m + \boldsymbol{\Delta\theta}^m$ and $|\boldsymbol{V}|^{m+1} = |\boldsymbol{V}|^m + \Delta|\boldsymbol{V}|^m$. The FDPF method approximates the Jacobian matrix using the following assumptions:

Assumption 1. *All lines have small resistances relative to their reactances. Thus,* $|G_{ik}/B_{ik}| \ll 1$, $\forall k \in \mathcal{N}_i$.

Assumption 2. *The voltage angle differences between connected buses* $(i,k) \in \mathcal{L}$ *are small, thus implying that* $\cos\theta_{ik} \approx 1$ *and* $\sin\theta_{ik} \approx \theta_{ik}$.

Assumption 3. *The voltage magnitude at each bus is approximately 1 pu.*

From Assumptions 1 and 2, the following approximations at bus $i \in \mathcal{N}$ are valid:

$$G_{ij} \approx 0\,; \quad G_{ij}\cos\theta_{ij} - B_{ij}\sin\theta_{ij} \approx 0\,; \quad \forall j \in \mathcal{N}_i. \tag{5}$$

With all these approximations, the real power is decoupled from the voltage magnitude and the reactive power is decoupled from the voltage angle as follows:

$$\frac{\boldsymbol{\Delta P}}{|\boldsymbol{V}|} \approx \boldsymbol{B'}\boldsymbol{\Delta\theta}, \tag{6a}$$

$$\frac{\boldsymbol{\Delta Q}}{|\boldsymbol{V}|} \approx \boldsymbol{B''}\boldsymbol{\Delta}|\boldsymbol{V}|, \tag{6b}$$

where $\boldsymbol{B'}$ and $\boldsymbol{B''}$ are constant matrices.[1] The decoupled relationships in (6) yield computational advantages as the $\boldsymbol{B'}$ and $\boldsymbol{B''}$ matrices are smaller in size than the Jacobian matrix $\boldsymbol{J}$ and are only factored once. The FDPF method iterates on (6a) and (6b) and then updates the mismatch by plugging the new values of voltage magnitudes and voltage angles into (2) [1].

III. Fast Decoupled Power Flow via Axis Rotation

This section formulates our proposed FDPF with axis rotation and presents our method for computing appropriate axis rotations ϕ_i at each bus $i \in \mathcal{N}$. As shown in Fig. 1, our axis rotation computations are implemented as a preprocessing step that occurs prior to the traditional FDPF method.

A. Axis Rotation

In the FDPF method, the line resistances are assumed to be much smaller than the line reactances (refer to Assumption 1). This assumption is not accurate when some lines have high R/X ratios. The concept of axis rotation (and a closely related variant known as *complex pu (cpu) normalization*) were introduced in [4]–[9] to address high R/X ratios.

Our proposed axis rotation approach multiplies both sides of (1) by the unit-magnitude complex parameter $e^{\mathbf{j}\phi_i}$:

$$S_i e^{\mathbf{j}\phi_i} = V_i(\sum_{k \in \mathcal{N}_i} Y_{ik} e^{-\mathbf{j}\phi_i} V_k)^*. \tag{7}$$

One technique for computing ϕ_i is by calculating the average angles of diagonal elements of the bus admittance matrix, i.e., $\phi_i = (1/n)\sum_{k \in \mathcal{N}} \arctan(-G_{kk}/B_{kk})$, for all $i \in \mathcal{N}$ [12]. However, in contrast to this technique, we allow

[1] We use the so-called XB version of the FDPF method [11].

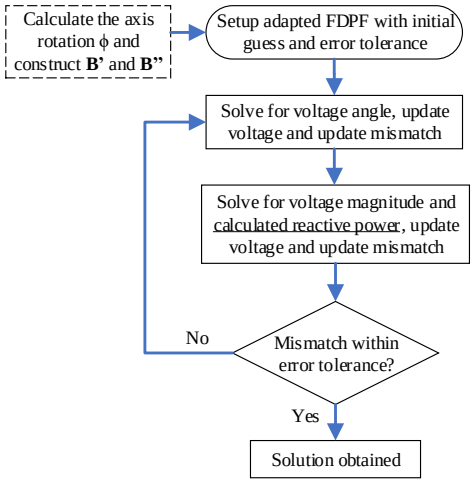

Fig. 1. Diagram of the FDPF method via multiple axis rotations. The dashed-line box is the axis rotation calculation representing our main addition to the traditional FDPF method. Our method also updates the calculated reactive power (underlined). The theta compensation can be added to the axis rotation before constructing constant matrices $\boldsymbol{B'}$ and $\boldsymbol{B''}$, if needed.

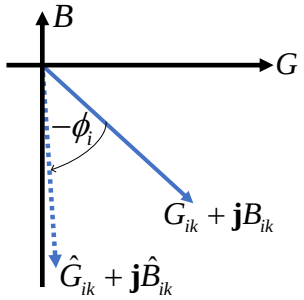

Fig. 2. The axis rotation of bus admittance.

for distinct values of ϕ_i at each bus i. Section III-C proposes our method for computing ϕ_i, $\forall i \in \mathcal{N}$.

The rotated real and reactive power injections are $\widehat{P}_i := P_i \cos\phi_i - Q_i \sin\phi_i$ and $\widehat{Q}_i := Q_i \cos\phi_i + P_i \sin\phi_i$, respectively. From (7), the power mismatch equations in (2) are:

$$\Delta\widehat{P}_i = \sum_{k\in\mathcal{N}_i} |V_i||V_k|(\widehat{G}_{ik}\cos\theta_{ik} + \widehat{B}_{ik}\sin\theta_{ik}) - \widehat{P}_i, \quad (8a)$$

$$\Delta\widehat{Q}_i = \sum_{k\in\mathcal{N}_i} |V_i||V_k|(\widehat{G}_{ik}\sin\theta_{ik} - \widehat{B}_{ik}\cos\theta_{ik}) - \widehat{Q}_i, \quad (8b)$$

where $\widehat{G}_{ik} = \mathrm{Re}(Y_{ik}e^{-\mathbf{j}\phi_i})$ and $\widehat{B}_{ik} = \mathrm{Im}(Y_{ik}e^{-\mathbf{j}\phi_i})$. We denote the rotated mismatch real (reactive) power as $\Delta\widehat{P}_i$ ($\Delta\widehat{Q}_i$). Fig. 2 shows how the bus admittance $\widehat{G}_{ik} + \mathbf{j}\widehat{B}_{ik} = Y_{ik}e^{-\mathbf{j}\phi_i}$ depends on the axis rotation.

Similar to (2), we aim to solve for the unknown voltage magnitudes and angles in (8) by reducing the rotated power mismatch to zero within a specified error tolerance.

B. Additional Reactive Power Balance Equation

As discussed in Section II, the traditional FDPF algorithm does not include reactive power balance equations at PV buses. However, since the axis rotation couples the real and reactive power injections at each bus, we must introduce a variable for the reactive power at PV buses along with an associated reactive power balance equation:

$$\Delta Q_{i,PV} = \sum_{k\in\mathcal{N}_i} |V_i||V_k|(G_{ik}\sin\theta_{ik} - B_{ik}\cos\theta_{ik}) - \widetilde{Q}_i, \quad (9)$$

where $\widetilde{Q}_i$ is a state variable corresponding to the reactive power injection at bus i. Hence, (6b) becomes:

$$\frac{\boldsymbol{\Delta Q}}{|\boldsymbol{V}|} \approx \left[\frac{\partial \boldsymbol{\Delta Q}/|\boldsymbol{V}|}{\partial \widetilde{\boldsymbol{Q}}},\ \boldsymbol{B''}\right]\begin{bmatrix}\widetilde{\boldsymbol{Q}}\\ \boldsymbol{\Delta}|\boldsymbol{V}|\end{bmatrix}, \quad (10)$$

where $\boldsymbol{B''}$ includes terms derived from (9). To maintain the square size of $\boldsymbol{B'}$ in (6a) with the decoupled relationships, we neglect the effect of $\widetilde{Q}_i$ on $\boldsymbol{B'}$. The additional reactive power equations have a small impact on the computation times since we factorize the associated matrices offline once and reuse them for all power flow problems solved for this system.

C. Axis Rotation via Minimizing the Sum of Squared Errors

In the FDPF method, the off-diagonal entries of the Jacobian matrix are approximated to be zero. They, in fact, are not zero and may be quite significant when Assumption 1 does not hold. This can lead the FDPF method to converge more slowly or fail to converge. Our approach minimizes the sum of the squared errors associated with the off-diagonal entries.

To analyze the errors caused by violations of Assumption 1, we start by looking at all four entries in the Jacobian matrix. Regarding to the construction of constant matrices in (6a) and (6b), the power mismatch is divided by the voltage magnitude to partially decouple the voltage magnitudes from the Jacobian matrix. For any pair of buses $i, j \in \mathcal{N}$, the entries of the Jacobian matrix, i.e., diagonal and off-diagonal entries are:

$$\frac{\partial \frac{\Delta P_i}{|V_i|}}{\partial\theta_j} = \begin{cases} -\sum\limits_{k\in\mathcal{N}_{i'}} |V_k|(G_{ik}\sin\theta_{ik} - B_{ik}\cos\theta_{ik}), & \text{if } i=j \\ |V_j|(G_{ij}\sin\theta_{ij} - B_{ij}\cos\theta_{ij}), & \text{otherwise.}\end{cases} \quad (11a)$$

$$\frac{\partial \frac{\Delta P_i}{|V_i|}}{\partial|V_j|} = \begin{cases} G_{ii}, & \text{if } i=j \\ G_{ij}\cos\theta_{ij} + B_{ij}\sin\theta_{ij}, & \text{otherwise.}\end{cases} \quad (11b)$$

$$\frac{\partial \frac{\Delta Q_i}{|V_i|}}{\partial\theta_j} = \begin{cases} \sum\limits_{k\in\mathcal{N}_{i'}} |V_k|(G_{ik}\cos\theta_{ik} + B_{ik}\sin\theta_{ik}), & \text{if } i=j \\ -|V_j|(G_{ij}\cos\theta_{ij} + B_{ij}\sin\theta_{ij}), & \text{otherwise.}\end{cases} \quad (11c)$$

$$\frac{\partial \frac{\Delta Q_i}{|V_i|}}{\partial|V_j|} = \begin{cases} -B_{ii}, & \text{if } i=j \\ \sum\limits_{k\in\mathcal{N}_{i'}} (G_{ik}\sin\theta_{ik} - B_{ik}\cos\theta_{ik}), & \text{otherwise.}\end{cases} \quad (11d)$$

The terms in (11a) and (11d) are the diagonal entries, while the terms in (11b) and (11c) are the off-diagonal entries. The expressions below show the off-diagonal entries at bus i with the axis rotation ϕ_i when Assumptions 2 and 3 hold:

$$F_{ij,P}(\phi_i) = G_{ij}\cos\phi_i + B_{ij}\sin\phi_i,\ j = 1,\ldots,n. \quad (12a)$$

$$F_{ij,Q}(\phi_i) = \begin{cases} \sum\limits_{k\in\mathcal{N}_{i'}} (G_{ik}\cos\phi_i + B_{ik}\sin\phi_i), & \text{if } i=j \\ -G_{ij}\cos\phi_i - B_{ij}\sin\phi_i, & \text{otherwise,}\end{cases} \quad (12b)$$

where $F_{ij,P}(\phi_i)$ and $F_{ij,Q}(\phi_i)$ are the rotated off-diagonal entries from (11b) and (11c), respectively. Since the error in

(12a) is different from (12b), we calculate the axis rotations for the real and reactive power mismatch equations separately.

We obtain the axis rotation for the real power mismatch equation at bus i, denoted as $\phi_{i,P}$, by minimizing the sum of the squared errors associated with each off-diagonal entry:

$$\phi_{i,P} = \underset{\phi_i}{\text{argmin}} \quad \sum_{j\in\mathcal{N}}(F_{ij,P}(\phi_i))^2. \tag{13}$$

The problem in (13) is solved analytically using the optimality condition for unconstrained optimization problems [13]:

$$\frac{\partial \sum_{j\in\mathcal{N}}(F_{ij,P}(\phi_i))^2}{\partial \phi_i} = 0. \tag{14}$$

From (14), the optimal solution to (13) is:

$$\phi_{i,P} = \frac{1}{2}\arctan\left(2\frac{\sum_{k\in\mathcal{N}_i} G_{ik}B_{ik}}{\sum_{k\in\mathcal{N}_i} G_{ik}^2 - B_{ik}^2}\right). \tag{15}$$

The solution in (15) is written in terms of the inverse tangent (arctan), which is periodic. To obtain small $\widehat{G}_{ik}$ and negative $\widehat{B}_{ik}$, we choose $0 \le \phi_{i,P} \le \pi/2$ (refer to Fig. 2).

The axis rotation for the reactive power mismatch equation at bus i, denoted as $\phi_{i,Q}$, is obtained similarly to (13). Specifically, we determine $\phi_{i,Q}$ via the optimality condition:

$$\begin{aligned}
&\sum_{k\in\mathcal{N}_{i'}}\Big((B_{ik}^2 - G_{ik}^2)\sin(2\phi_{i,Q}) + 2B_{ik}G_{ik}\cos(2\phi_{i,Q})\Big) \\
&\quad + 2\cos(2\phi_{i,Q})\sum_{k\in\mathcal{N}_{i'}} B_{ik}\cdot\Big(\sum_{k\in\mathcal{N}_{i'}} G_{ik}\Big) \\
&\quad + \sin(2\phi_{i,Q})\Big(\Big(\sum_{k\in\mathcal{N}_{i'}} B_{ik}\Big)^2 - \Big(\sum_{k\in\mathcal{N}_{i'}} G_{ik}\Big)^2\Big) = 0.
\end{aligned} \tag{16}$$

Solving (16) yields:

$$\phi_{i,Q} = \frac{1}{2}\arctan\left(2\frac{\sum_{k\in\mathcal{N}_{i'}} G_{ik}B_{ik} + \sum_{k\in\mathcal{N}_{i'}} B_{ik}\sum_{k\in\mathcal{N}_{i'}} G_{ik}}{\sum_{k\in\mathcal{N}_{i'}}\left(G_{ik}^2 - B_{ik}^2\right) + \Big(\sum_{k\in\mathcal{N}_{i'}} G_{ik}\Big)^2 - \Big(\sum_{k\in\mathcal{N}_{i'}} B_{ik}\Big)^2}\right). \tag{17}$$

Similar to $\phi_{i,P}$, we choose $0 \le \phi_{i,Q} \le \pi/2$. The solutions obtained from (15) and (17) rotate the bus admittance Y_{ik} such that the absolute value of the rotated conductance $\widehat{G}_{ik}$ is small to improve the FDPF method's approximation accuracy. By explicitly minimizing the error in the off-diagonal entries of the Jacobian approximation used by the FDPF, our method for choosing the axis rotations also directly reduces the error caused by assuming small R/X ratios in the diagonal entries.

As shown in Fig. 1, we proceed similarly to the usual FDPF method after computing the axis rotations from (15) and (17).

D. Analysis of Large Angle Difference

The method described above for computing values for ϕ_i relies on the small angle difference approximation from Assumption 2. We next consider cases where this assumption does not hold, i.e., $\theta_{ik} \not\approx 0$ for some line $(i,k) \in \mathcal{L}$. In order to continue applying the small angle approximation, we introduce an additional axis rotation to compensate for the large voltage angle difference (so-called *theta compensation*). The theta compensation Θ_i is computed by assuming that a good estimate of the voltage angle at each bus is known.[2] Given the approximated angle differences for each line, $\overline{\theta}_{ik}\,; \forall (i,k) \in \mathcal{L}$, the theta compensation at bus i is:

$$\Theta_i = \frac{\sum_{k\in\mathcal{N}_{i'}} \overline{\theta}_{ik}}{N_i}, \tag{18}$$

where N_i is the number of lines connected to bus i. The complex power balance equation (7) becomes:

$$S_i e^{\mathbf{j}(\phi_i - \Theta_i)} = V_i\Big(\sum_{k\in\mathcal{N}_i} Y_{ik}e^{-\mathbf{j}(\phi_i-\Theta_i)}V_k\Big)^*. \tag{19}$$

From (19), the power balance equations (8a) and (8b) with theta compensation become:

$$\begin{aligned}
\Delta\breve{P}_i &= \sum_{k\in\mathcal{N}_i}|V_i||V_k|(\widehat{G}_{ik}\cos(\theta_{ik}-\Theta_i) + \widehat{B}_{ik}\sin(\theta_{ik}-\Theta_i)) \\
&\quad - (\widehat{P}_i\cos\Theta_i + \widehat{Q}_i\sin\Theta_i),
\end{aligned} \tag{20a}$$

$$\begin{aligned}
\Delta\breve{Q}_i &= \sum_{k\in\mathcal{N}_i}|V_i||V_k|(\widehat{G}_{ik}\sin(\theta_{ik}-\Theta_i) - \widehat{B}_{ik}\cos(\theta_{ik}-\Theta_i)) \\
&\quad - (\widehat{Q}_i\cos\Theta_i - \widehat{P}_i\sin\Theta_i),
\end{aligned} \tag{20b}$$

where $\Delta\breve{P}_i$ ($\Delta\breve{Q}_i$) is the rotated real (reactive) power mismatch with the theta compensation.

Let $\mathrm{sgn}(\cdot)$ denote the sign function. Since the angle differences $\overline{\theta}_{ik}$ can be positive, negative, or zero, applying theta compensation Θ_i is most beneficial when the values of $\mathrm{sgn}(\overline{\theta}_{ik})$ are the same for all $k \in \mathcal{N}_{i'}$. From the DC power flow approximation, $\mathrm{sgn}(\overline{\theta}_{ik})$ often identifies the direction of real power flow [14]. Thus, values for $\mathrm{sgn}(\overline{\theta}_{ik})$ are usually the same for all $k \in \mathcal{N}_{i'}$ when real power either flows out from bus i to all neighboring buses or flows from all neighboring buses into bus i.

IV. Simulation and Results

This section uses a variety of test cases to demonstrate the proposed axis rotation method's ability to improve the convergence characteristics of the FDPF method. First, we compare the effect of multiple axis rotations in the FDPF method for cases where the line R/X ratios are high to cases where the line R/X ratios are low. We compare the performance of traditional FDPF and our proposed axis rotation FDPF method in terms of the number of iterations required to achieve a tolerance of 10^{-6}. Second, we present a comparison of the convergence performance from our method to the method with the single axis rotation. Last, we demonstrate the effectiveness of our proposed method in a system that has large voltage angle differences. We performed our numerical experiments by adopting code and selected test cases from MATPOWER [15].

[2]Methods for estimating the angle differences include using the solution to a related problem, solving the DC power flow, or examining historical data.

TABLE I
NUMBER OF ITERATIONS OF FDPF WITH DIFFERENT ϕ AT EACH BUS COMPARED TO TRADITIONAL FDPF FOR DISTRIBUTION SYSTEMS.

Case	FDPF	FPDF with multiple axis rotations
case33bw	9	6
case69	13	6
case85	13	7

TABLE II
NUMBER OF ITERATIONS OF FDPF WITH DIFFERENT ϕ AT EACH BUS COMPARED TO TRADITIONAL FDPF FOR TRANSMISSION SYSTEMS.

Case	FDPF	FDPF with multiple axis rotations	Increased Resistance	
			FDPF	FDPF with multiple axis rotations
case9	6	6	9	8
case14	6	6	17	10
case30	8	6	15	7
case_ieee30	6	6	18	11
case39	7	8	22	18
case89pegase	7	7	14	11
case118	8	7	20	13

A. Effect of Axis Rotations

We first numerically test the axis rotations using ten systems (three distribution and seven transmission systems). We compare our proposed method with the traditional FDPF method.

Another set of tests is conducted to validate the efficiency of our proposed method using modified transmission systems that are more lossy than the original systems, leading to larger axis rotations. For these tests, all line resistance values are increased by 40% of their reactance values, i.e., $R_{\text{new}} = R + 0.4X$, where R_{new} is the increased resistance.

Table I shows the simulation results from the distribution systems, which have high R/X ratios. The axis rotations introduced by our method effectively reduce the FDPF approximation errors. Our method requires significantly fewer iterations than the traditional FDPF method (percentage reductions of 33%, 54% and 46% for *case33bw*, *case69*, and *case85*).

Table II shows the simulation results for the transmission systems. With the exception of *case39* where our method takes one additional iteration, our proposed method requires the same number or fewer iterations for all considered test cases. However, the improvements are modest (reductions of one or two iterations) for cases with low R/X ratios. For cases with increased resistance values, our method converges significantly faster than the traditional FDPF method, with reductions in the number of iterations ranging from 11% to 53%.

B. Multiple Axis Rotations vs. Single Axis Rotation

We next compare our proposed method to methods in previous papers that use one axis rotation for the entire system or subsystem [4]–[7], [9]. For the single axis rotation, we choose the average angles of diagonal elements of the bus admittance matrix as suggested by [12]. We consider a 3-bus system based on *case3_lmbd* [16], a 4-bus system based on *case4gs* [15], and a 5-bus system based on *case5* [15]. These systems are described in the appendix (Table V).

TABLE III
MULTIPLE AXIS ROTATIONS VS. SINGLE AXIS ROTATION: AXIS ROTATION AND NUMBER OF ITERATIONS FOR THE 3-, 4-, AND 5-BUS SYSTEMS.

		3-bus system	4-bus system	5-bus system
Axis rotation	Multiple axis rotations	27.8°, 3.8°, 26.3°	25.7°, 25.7°, 40.6°, 40.6°	40.5°, 8.0°, 7.9°, 33.0°, 45.0°
	Single axis rotation	21.4°	33.3°	27.0°
Number of iterations	Multiple axis rotations	15	6	8
	Single axis rotation	18	8	11
	FDPF	25	11	22

Table III shows the axis rotations for the real power equations at each bus, $\phi_{i,P}$, calculated from (15) and the number of iterations for all three systems. Note that the angles for the reactive power equations, $\phi_{i,Q}$, calculated from (17) are similar to (15). The angles have a large spread, ranging from 3.8° to 45.0°. The results in Table III validate the efficiency of our method. With the single axis rotation for the entire system, the percentage reductions in the number of iterations are 28%, 27.27%, and 50% for 3-, 4-, and 5-bus systems, respectively. By applying the multiple axis rotations, the percentage reductions in the number of iterations go up to 40%, 45.45%, and 63.63% for 3-, 4-, and 5-bus systems, respectively. Allowing each bus to have different axis rotations thus results in faster convergence.

C. Large Voltage Angle Difference

Consider a system that has large voltage angle differences between some connected buses. Four test cases are created based on the 3-bus system shown in Fig. 3. Case 1 and Case 3 have all lines as shown in Fig. 3, where Case 2 and Case 4 remove the line connecting buses 2 and 3 (dashed line). All lines in Case 1 and Case 2 are lossless. Table VI in the appendix provides the system parameters. The theta compensation is calculated via (18) under the assumption that good estimates of all voltage angles are known.

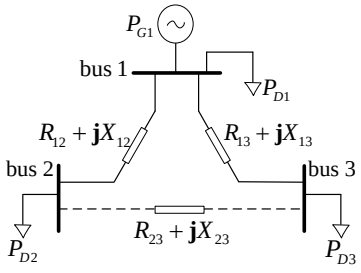

Fig. 3. The 3-bus system with one generator and two loads. The line impedance connecting bus i to bus k is expressed as $R_{ik} + \mathbf{j}X_{ik}$.

Table IV presents the number of iterations for all cases. In Case 1 and Case 3, note that the line flows bring power both into and out of bus 3. As discussed in Section III-D,

TABLE IV
NUMBER OF ITERATIONS OF FDPF WITH A DIFFERENT ϕ AT EACH BUS COMPARED TO TRADITIONAL FDPF IN CASES WITH LARGE VOLTAGE ANGLE DIFFERENCES.

		Case 1	Case 2	Case 3	Case 4
Method* (Number of iterations)**	#1	12	68	16	17
	#2	12†	68†	13	14
	#3	11	13	11	6

***Method #1: traditional FDPF. Method #2: FDPF with the multiple axis rotations, but no theta compensation. Method #3: modified FDPF with multiple axis rotations and theta compensation.
†Since all lines are lossless for these cases, method #2 takes the same number of iterations as method #1.

theta compensation at bus 3 is not very beneficial for this case, as validated by the modest improvements in the number of iterations for these cases. Conversely, Case 2 and Case 4 show the significant improvements from applying the theta compensation. The axis rotation without theta compensation also improves convergence in Case 3 and Case 4. Note that the convergence performance depends on the accuracy of the voltage angles used to compute the theta compensation.

V. CONCLUSION AND FUTURE WORK

The FDPF method exhibits convergence challenges in systems with high R/X ratios, e.g., distribution and some sub-transmission systems. This paper has formulated and analyzed an axis rotation method that addresses these convergence challenges. Our numerical tests show the effectiveness of the proposed method over the traditional FDPF, especially when lines have high R/X ratios. Furthermore, allowing for different axis rotations at each bus can lead to significantly improved convergence performance relative to prior methods that use a single axis rotation, particularly when the lines' R/X ratios widely vary across the system.

Our future work aims to develop alternative algorithms for calculating the axis rotations in order to further improve the convergence characteristics. Additionally, we will extend our method to three-phase network models in order to further study joint transmission/distribution power flow problems.

APPENDIX

In Tables V and VI, this appendix describes the 3-, 4-, and 5-bus test cases analyzed in Sections IV-B and IV-C.

TABLE V
LINE PARAMETERS FOR 3-, 4-, AND 5-BUS SYSTEMS IN SECTION IV-B.

3-bus system	**From-to**		
	1-2	**1-3**	**2-3**
R (pu)	0.042	0.65	0.05
X (pu)	0.9	0.62	0.75

4-bus system	**From-to**			
	1-2	**1-3**	**2-4**	**3-4**
R (pu)	0.01008	0.02976	0.02976	0.0636
X (pu)	0.0504	0.0372	0.0372	0.0636

5-bus system	**From-to**					
	1-2	**1-4**	**1-5**	**2-3**	**3-4**	**4-5**
R (pu)	0.00843	0.0304	0.0064	0.00108	0.00891	0.0297
X (pu)	0.0281	0.0304	0.0064	0.0108	0.0297	0.0297

TABLE VI
3-BUS SYSTEM PARAMETERS FOR FOUR SPECIFIED TEST CASES IN SECTION IV-C.

		Case 1	Case 2	Case 3	Case 4
Line Impedance (pu) /From-to	1-2	$\mathbf{j}0.9$	$\mathbf{j}0.9$	$0.3+\mathbf{j}0.9$	$0.3+\mathbf{j}0.9$
	1-3	$\mathbf{j}0.62$	$\mathbf{j}0.62$	$0.3+\mathbf{j}0.62$	$0.3+\mathbf{j}0.62$
	2-3	$\mathbf{j}0.75$	-	$0.3+\mathbf{j}0.75$	-
Bus angle**	Bus 2	-54.1°	-81.9°	-32.8°	-38.5°
	Bus 3	-45.5°	-36.1°	-29.6°	-25.4°
Power Demand (MVA)	P_{D1}	$117.5\angle$ 20.0°		$68.0\angle$ 36.0°	
	P_{D2}	$117.5\angle$ 20.0°		$68.0\angle$ 36.0°	
	P_{D3}	$107.4\angle$ 27.8°		$70.7\angle$ 45.0°	

**Bus 1 is the reference bus, and thus its angle is zero.

REFERENCES

[1] B. Stott and O. Alsac, "Fast decoupled load flow," *IEEE Trans. Power Appar. Syst.*, vol. PAS-93, no. 3, pp. 859–869, May 1974.

[2] F. F. Wu, "Theoretical study of the convergence of the fast decoupled load flow," *IEEE Trans. Power Appar. Syst.*, vol. 96, no. 1, pp. 268–275, Jan. 1977.

[3] J. Nanda, D. Kothari, and S. Srivastava, "Some important observations on fast decoupled load flow algorithm," *Proc. IEEE*, vol. 75, no. 5, pp. 732–733, May 1987.

[4] B. Sirait and J. Irisawa, "Fast decoupled load flow via axis rotation," Nagaoka Unversity of Technolgy, Tech. Rep. #17, May 1995. [Online]. Available: https://lib.nagaokaut.ac.jp/kiyou/data/study/k17/K17_4.pdf

[5] T. Ochi, D. Yamashita, K. Koyanagi, and R. Yokoyama, "The development and the application of fast decoupled load flow method for distribution systems with high r/x ratios lines," in *IEEE PES Innovative Smart Grid Technologies Conf. (ISGT)*, Feb. 2013, pp. 1–6.

[6] E. M. Lourenço, T. Loddi, and O. L. Tortelli, "Unified load flow analysis for emerging distribution systems," in *IEEE PES Innovative Smart Grid Technologies Conf. Europe (ISGT Europe)*, Oct. 2010, pp. 1–7.

[7] C. C. Durce, O. L. Tortelli, E. M. Lourenco, E. M. Lourenço, and T. Loddi, "Complex normalization to perform power flow analysis in emerging distribution systems," in *3rd IEEE PES Innovative Smart Grid Technologies Europe (ISGT Europe)*, Oct. 2012, pp. 1–6.

[8] O. L. Tortelli, E. M. Lourenço, A. V. Garcia, and B. C. Pal, "Fast decoupled power flow to emerging distribution systems via complex pu normalization," *IEEE Trans. Power Syst.*, vol. 30, no. 3, pp. 1351–1358, May 2015.

[9] R. K. Portelinha, C. C. Durce, O. L. Tortelli, E. M. Lourenço, and B. C. Pal, "Unified Transmission and Distribution Fast Decoupled Power Flow," *J. Control, Automat. Electr. Syst.*, vol. 30, no. 6, pp. 1051–1058, Dec. 2019.

[10] W. F. Tinney and C. E. Hart, "Power flow solution by Newton's method," *IEEE Trans. Power Appar. Syst.*, vol. PAS-86, no. 11, pp. 1449–1460, Nov. 1967.

[11] X.-F. Wang, Y. Song, and M. Irving, *Modern Power Systems Analysis*. Springer Science & Business Media, Jun. 2010.

[12] P. H. Haley and M. Ayres, "Super decoupled loadflow with distributed slack bus," *IEEE Trans. on PAS*, vol. PAS-104, no. 1, pp. 104–113, Jan. 1985.

[13] A. Beck, *Introduction to Nonlinear Optimization: Theory, Algorithms, and Applications with MATLAB*. Philadelphia, PA: Society for Industrial and Applied Mathematics, Oct. 2014.

[14] K. Purchala, L. Meeus, D. Van Dommelen, and R. Belmans, "Usefulness of DC power flow for active power flow analysis," in *IEEE PES General Meeting*, June 2005, pp. 454–459.

[15] R. D. Zimmerman, C. E. Murillo-Sánchez, and R. J. Thomas, "MATPOWER: Steady-State Operations, Planning, and Analysis Tools for Power Systems Research and Education," *IEEE Trans. Power Syst.*, vol. 26, no. 1, pp. 12–19, Feb. 2011.

[16] IEEE PES PGLib-OPF Task Force, "The power grid library for benchmarking AC optimal power flow algorithms," Aug. 2019, arXiv:1908.02788.